

POLARIZATION ANGLE EFFECT ON HIGH-ORDER HARMONIC GENERATION IN AN INHOMOGENEOUS TWO-COLOR LASER FIELD

Stephen Maina Njoroge^{1*}

Biological and Physical Sciences Department, Karatina University, 1957-10101 Karatina, Kenya *snjoroge@karu.ac.ke

Received 2025-02-26, Revised 2025-08-13, Accepted 2025-09-24, Available Online 2025-10-1, Published Regularly October 2025

ABSTRACT

High-order harmonic generation (HHG) has emerged as a promising route for producing coherent extreme ultraviolet (XUV) radiation and attosecond pulses. The enhancement of harmonic yield and extension of the cutoff energy are key challenges, particularly when using conventional homogeneous fields. Recent theoretical and experimental studies have shown that combining two-color laser fields with spatial inhomogeneities can significantly improve HHG efficiency. However, the effect of polarization angle on this process remains insufficiently explored. This study theoretically investigates HHG driven by a two-color inhomogeneous field using the strong-field approximation (SFA) framework. Numerical simulations were performed to analyze harmonic spectra under varying polarization angles, comparing one-color and two-color configurations. The role of the inhomogeneity parameter was also examined to determine its influence on supercontinuum generation and cutoff extension. The simulations revealed that the introduction of two-color fields enhanced the harmonic cutoff from the 70th to the 90th order compared with a one-color homogeneous field. Incorporating an inhomogeneity parameter of 0.003 further broadened the harmonic spectrum, producing a supercontinuum spanning approximately 270 orders. However, increasing the polarization angle from 0.0π to 0.5π resulted in a noticeable reduction of the harmonic cutoff, thereby limiting the generation of high-energy harmonics. These findings demonstrate that two-color inhomogeneous fields provide an effective means of extending the harmonic cutoff and generating broadband supercontinua suitable for attosecond pulse synthesis. Nevertheless, careful control of the polarization angle is essential, as misalignment significantly suppresses HHG efficiency. The study highlights the importance of polarization engineering in optimizing HHG sources for applications in ultrafast science and spectroscopy.

Key words: supercontinuum; polarization angle; high-order harmonic generation; harmonic spectrum

INTRODUCTION

When atoms or molecules are irradiated by an intense laser field three nonlinear phenomena can be initiated; high order harmonic generation (HHG), above threshold ionization (ATI) and non-sequential double ionization (NSDI) ^[1, 2]. However, HHG phenomenon has generated much research interest in recent years owing to numerous noble applications ^[3, 4]. First, HHG is utilized in the generation of a coherent light source in the spectral range of ultraviolet (UV) to extreme ultraviolet (EUV) range ^[5, 6]. In addition, it has proven to be an appropriate technique in the experimental and theoretical generation of coherent attosecond pulses. This is a reliable pathway

to the extraction of both spatial and temporal information with extremely high resolution ^[7, 8]. Conceptually, the process of HHG is well elaborated by three steps or a 'simple man' model ^[9]. First, under the influence of very strong laser field bound, electron tunnel through coulomb potential. The freed electron is accelerated in the laser field and recombines at a later time with

parent ion emitting a photon with energy $I_p + 3.17U_p$; I_p is ionization potential and $U_p \alpha I \lambda^2$ is ponderomotive energy. These processes are repetitive at every half cycle of the laser field and contribute to two major electron trajectories: long and short electron trajectories [10-13]. Each electron trajectory yields an attosecond pulse at every half optical cycle resulting to generation of attosecond pulse train (APT). However, for practical applications, an isolated attosecond pulse (IAP) is of paramount importance [7, 14]. This has triggered the emergence of different schemes with the objective of generating IAPs. They include and are not limited to: few-cycle pulse [15], polarization gating [16], two-color or multi-color [13, 17-21], chirped pulse [22, 23], and static field controlling scheme [24].

Recently, a new technique known as plasmonic field enhancement has brought a paradigm shift in HHG. The scheme has attracted much attention both experimentally ^[25] and theoretically ^[26-29]. Using the scheme, a low-femtosecond oscillator can be used to generate HHG without the addition of an extra cavity in order to amplify laser intensity. This is realized by illuminating metallic nanostructures or nanoparticles with a low-intensity pulse; the intensity can be enhanced by more than 20 dB ^[30]. As a result, the threshold of laser intensity for HHG in inert gases is surpassed. In addition, pulse repetition remains constant in the process. The harmonic radiation from each nanostructure acts as a point source, thus enabling the focusing of coherent radiation ^[30–33].

To diversify practical applications of IAPs, control of IAP properties such as frequency, phase, polarization, and amplitude is critically important ^[21, 34, 35]. Since the mean frequency of IAPs is in the spectral range of UV or EUV, where optical elements are not readily available to control polarization ^[36], such control must be established during generation. Full control of polarization has been achieved by adjusting the ellipticity of the counter-rotating few-cycle pulse for non-collinear HHG ^[37]. Ruiz et al. have demonstrated polarization control of APT using an orthogonally polarized two-color scheme. This is achieved via control of the carrier envelope phase. An investigation on the polarization of attosecond pulses generated by two-color circularly polarized pulses has been done ^[38]. Furthermore, a scheme of linear perpendicular fields was proposed to control the polarization angle of the harmonic ^[39]. To date, the use of two-color fields has emerged as one of the ways of increasing the harmonic cutoff, resulting in a broadband XUV as well as the selection of a short quantum path continuum. However, detailed information on the polarization orientation of the two-color fields has not been adequately addressed.

In this paper, we theoretically demonstrate the effect of polarization angle in an inhomogeneous two-color field on high-order harmonic generation. Based on the results obtained by solving the time-dependent Schrödinger equation, we demonstrate that high-order harmonic generation can be controlled better by using two color fields over one color field. Moreover, we have investigated the influence of polarization angle on the generated harmonic spectrum. The results show that by increasing polarization angle 0.0π from to 0.5π , the spectrum is characterized by reduction of plateau region and low harmonic yield.

Theoretical Model

The theoretical investigation was carried out using MATLAB R2023a version as the primary computational environment. MATLAB was chosen because of its robust numerical solvers, fast Fourier transform (FFT) capabilities, and ability to efficiently handle time-dependent simulations of electron dynamics in strong fields. The simulation of the HHG spectra was by solving the two-dimensional time-dependent Schrödinger equation (2D-TDSE). The 2D-TDSE is given by (throughout this paper atomic unit (a.u) are used unless stated otherwise)

$$i\frac{\partial \psi(x,y,t)}{\partial t} = H(x,y,t)\psi(x,y,t)$$

$$= \left[-\frac{1}{2}\frac{\partial^{2}}{\partial x^{2}} - \frac{1}{2}\frac{\partial^{2}}{\partial y^{2}} + V_{a}(x,y) + V_{l}(x,y,t) \right]\psi(x,y,t). \tag{1}$$

Where $V_a(x) = -1/(\alpha + x^2 + y^2)^{1/2}$ is the soft coulomb potential with α =0.1195 to match ionization potential for the ground state of Ne 0.7925a.u and $V_l(x,t)$ is potential due to the interaction between laser and electron. The inhomogeneous field along x- component is expressed as

$$E_{x}(x,t) = E_{xt}(t)(1 + \varepsilon_{x}x),$$

$$E_{y}(y,t) = E_{yt}(t)(1 + \varepsilon_{y}y).$$
(2)

and ε is the spatial inhomogeneity of the laser field [40, 41]. The synthesized laser field is expressed as,

$$E_{xt}(t) = E_0 f(t) \cos(\omega_0 t + \phi_0) + E_1 f(t) \cos(\omega_1 t + \phi_1 - \Delta \phi) \cos \theta,$$

$$E_{yt}(t) = E_1 f(t) \cos(\omega_1 t + \phi_1 - \Delta \phi) \sin \theta.$$
(3)

Here E_0 , E_1 , $^{\omega_0}$ and $^{\omega_1}$ are the amplitude and frequencies of fundamental pulse and control pulse respectively. $^{\phi_0}$ and $^{\phi_1}$ are CEPs of fundamental pulse and control pulse whereas $^{\Delta\phi}$ is the relative phase between the two pulses. $^{\theta_0}$ is the orientation angle between the two fields. The envelope function is $f(t) = \sin^2(\pi t/T)$, $T = 10T_0$, T_0 represent the optical cycle of the fundamental pulse. The solution to equation (1) is obtained by the use of a split operator method $^{[42]}$. The time-dependent dipole acceleration is expressed as

$$a_{x}(t) = -\langle \psi(x, y, t) | [H(x, y, t), [H(x, y, t), x]] \psi(x, y, t) \rangle,$$

$$a_{y}(t) = -\langle \psi(x, y, t) | [H(x, y, t), [H(x, y, t), y]] \psi(x, y, t) \rangle.$$
(4)

Whereas the harmonic spectrum is generated by applying the Fourier transform on time-dependent dipole acceleration,

$$\left|s_{qx}(\omega)\right|^{2} = \left|\frac{1}{T}\int_{0}^{T} a_{x}(t)e^{-iq\omega t}dt\right|^{2},$$

$$\left|s_{qy}(\omega)\right|^{2} = \left|\frac{1}{T}\int_{0}^{T} a_{y}(t)e^{-iq\omega t}dt\right|^{2}.$$
(5)

Here q is the harmonic order. The obtained harmonics are in the frequency domain. Therefore, to obtain the detailed spectral and temporal structures of HHG at each half optical cycle in time, we

performed time-frequency analysis or spectrogram of the field by means of the wavelet transform [43, 44]

$$A(t_0,\omega) = \int a(t)\sqrt{\omega}W(\omega(t-t_0))dt$$
 (6)

Where $W(\omega(t-t_0))_{is}$ the Morlet wavelet expressed as [58]

$$W(\xi) = \left(\frac{1}{\sqrt{\tau}}\right) e^{i\xi} e^{-\xi^2/2\tau^2} \tag{7}$$

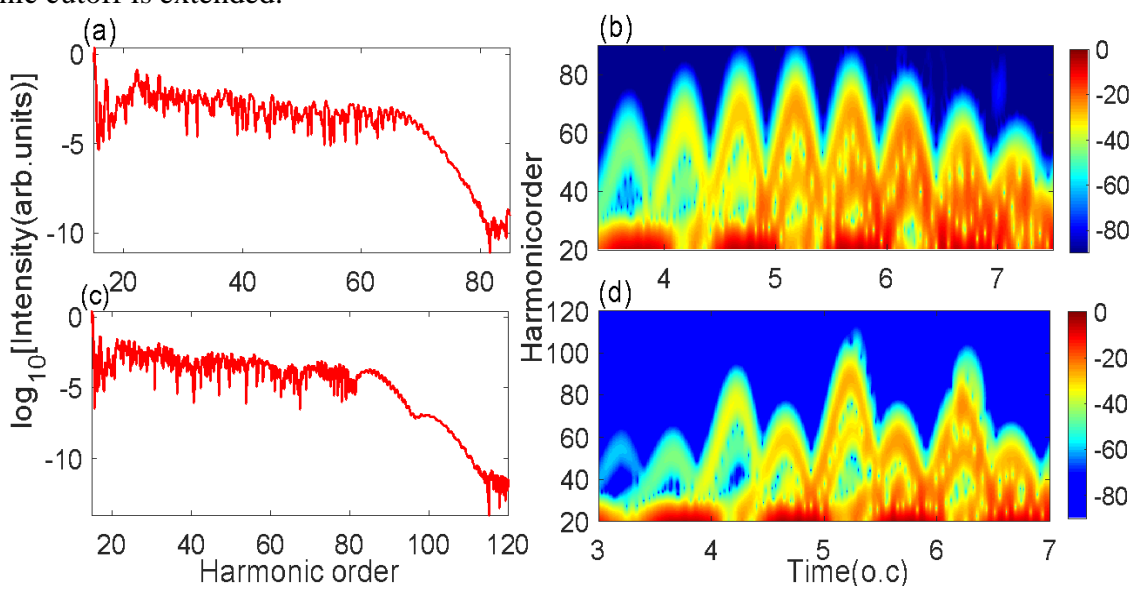
It is worth mentioning that the width of window function in the wavelet transform varies with respect to frequency. However, the number of oscillations within the window was maintained at a constant value.

Results and discussion

Fig. 1 (a) and (b) show the calculated one-color field (10 fs/800 nm) harmonic spectrum and the corresponding spectrogram distribution, respectively. Fig. 1(b) clearly illustrates that within each half optical cycle, there exist two distinct branches of comparable intensity: short and long quantum paths. As a result of the interference of the quantum paths, the harmonic spectrum exhibits large modulation structures in the plateau (flat-intensity) region in the harmonic spectrum with a cutoff at 70th order [see Fig. 1(a)]. Figs. 1 (c) and (d) show the linearly polarized two-color field harmonic spectrum and its corresponding spectrogram, respectively synthesized by a 10 fs/800 nm driving pulse and a 10 fs/2000 nm control pulse. The intensities of these two laser pulses are chosen to be $3.0 \times 10^{14} \text{W/cm}^2$ and $6.0 \times 10^{13} \text{W/cm}^2$, respectively. In Fig. 1(d), one can see that

above 80th orders there exist three noticeable peaks at approximately 4T_0 , 5T_0 and 6T_0 . The

intensity of the peak at 5T_0 is the highest thus it is the one that mainly contribute to the harmonic cutoff of 90th in the spectrum [see Fig. 1(c)]. The inhomogeneity parameter in this case was assumed to be ε =0.00. Comparing Figs. 1(a) and (c), one can see that the two-color field spectrum has low modulation structures in the plateau region than the one-color field. Moreover, the harmonic cutoff is extended.



Copyright © 2025 Universitas Sebelas Maret

Figure 1: (a) and (b) The harmonic spectrum and the corresponding spectrogram in the one-color field, respectively. (c) and (d) Same as (a) and (b) in the two-color field. The intensities of the 800nm and 2000 nm are $3.0x10^{13}$ W/cm² and $6.0x10^{13}$ W/cm², respectively. Here the inhomogeneity parameter was taken to be ε =0.00.

We investigated the effect of the inhomogeneity parameter in a linearly polarized two-color field as presented in Fig. 2 (the inhomogeneous parameter was similar for the two fields). Figs. 2 (a) and (b) illustrates harmonic spectrum and the corresponding spectrogram, respectively with inhomogeneity parameter ε =0.00 (the case of homogeneous field). As can be clearly observed from Fig. 2 (b) that harmonic above 105th to 140th orders are dominated by three peaks at

approximately ${}^{5}T_{0}$, ${}^{6}T_{0}$ and ${}^{6.5}T_{0}$. The intensity of the peak at ${}^{6.5}T_{0}$ is higher than the other two peaks hence it is the one that mainly contribute to the double plateau region in the harmonic spectrum shown in Fig. 2 (a). When the inhomogeneity parameter is increased to ε =0.001, the cutoff is extended to about 200th order as shown in Fig 2 (c) and (d). In Fig. 2 (d) one can see that harmonic above 130th to 160th orders are dominated by a single peak followed by two branches

of equal intensity between 160th to 200th orders at approximately ${}^{5}T_{0}$. For this reason, the harmonic spectrum shown in Fig. 2 (d) is characterized by a smooth plateau between 130th to 160th orders and modulation structure between 160th to 200th orders due to interference of the quantum paths. On increasing the inhomogeneity parameter to ε =0.002 [Figs. 2 (e) and (f)], the harmonic cutoff is extended to 310th order. One can see that only short quantum path survives leading to generation of a smooth supercontinuum (continuous spectral region) with a broad bandwidth of about 150th orders [see Fig. 2 (e)]. On increasing the inhomogeneity parameter to

 ε =0.003, only one maximum radiation peak at 5T_0 is observed as shown in Fig. 2 (h) with the highest radiation of 415th order which is 265th orders higher than the second highest radiation. Therefore, abroad supercontinuum is generated from 150th to 415th orders as presented in Fig. 2 (g). It is clear that increasing the inhomogeneity parameter resulted to generation of a smooth supercontinuum with a remarkable extension of the harmonic cutoff.

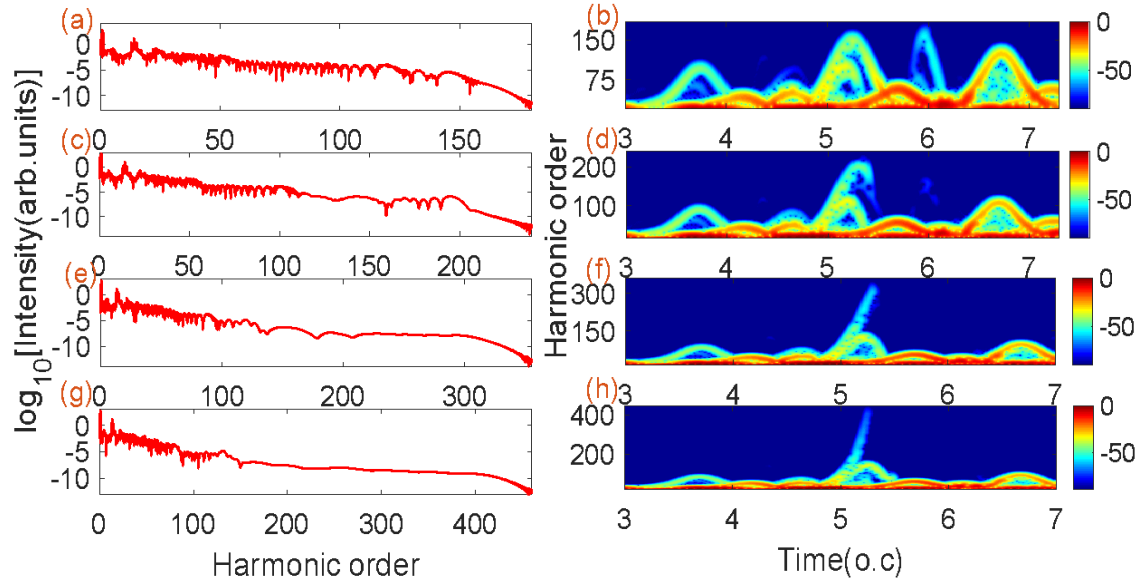


Figure 2: (a) and (b) The harmonic spectrum and the corresponding spectrogram in the homogeneous two-color field, respectively. (c) and (d), (e) and (f), (g) and (h) same as (a) and (b) in the inhomogeneous two-color field with inhomogeneity parameter 0.001, 0.002 and 0.003, respectively. Here the polarization angle of the laser

field is 0.0π and inhomogeneity parameter was similar for the two fields.

In Fig. 3 (a) we present the effect of varying the wavelength of the control pulse on the harmonic emission. Apart from the variation of the control pulse wavelength, other parameters are as in Fig. 2 (g). Here we choose control pulse wavelength 800nm (red line), 1200nm (green line), 1600nm (blue line), 2000nm (black line) and 2400nm (pink line). One can clearly see that on increasing the control pulse wavelength the harmonic cutoff is extended and modulation structure eliminated. This observation is as a result of abrupt reduction of the central frequency of the control laser field. Figure 3 (b) shows the effect of varying the intensity of the control pulse. Here the intensity of the control pulse is chosen to be $1.5 \times 10^{13} \text{W/cm}^2$ (green line), $3.0 \times 10^{13} \text{W/cm}^2$ (blue line), $4.5 \times 10^{13} \text{W/cm}^2$ (black line) and $6.0 \times 10^{13} \text{W/cm}^2$ (red line). One can see that on increasing the control pulse intensity the harmonic cutoff is gradually extended. This implies that by choosing a high intense control pulse it's the surest test of obtaining a broad supercontinuum. However, a combination of long wavelength control pulse with high intensity cannot be easily realized in experiment.

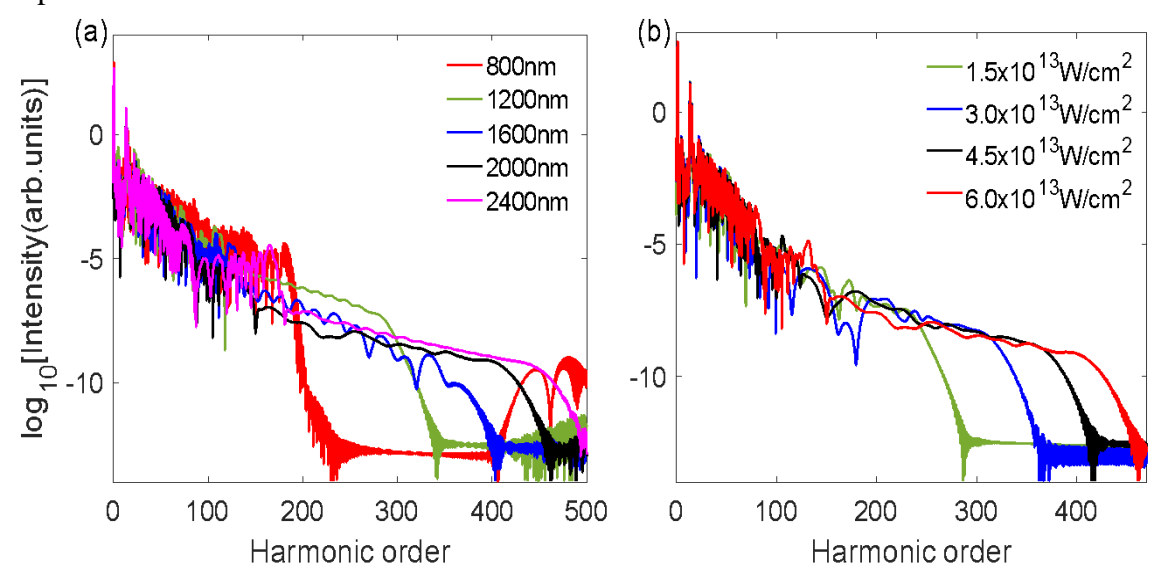


Figure 3: (a) Variation of the control pulse wavelength. Red line (800nm), green line (1200nm), blue line (1600nm), black line (2000nm) and pink line (2400nm) (b) Variation of control pulse intensity. $1.5 \times 10^{13} \text{W/cm}^2$ (green line), $3.0 \times 10^{13} \text{W/cm}^2$ (blue line), $4.5 \times 10^{13} \text{W/cm}^2$ (black line) and $6.0 \times 10^{13} \text{W/cm}^2$ (red line). Here inhomogeneous two-color field is used. The polarization angle between the control pulse and the driving pulse is 0.0π .

Figure 4 shows the calculated harmonic spectra driven by the two-color fields having cross linear polarization in a homogeneous field. Here we varied the polarization angle. One can clearly see that for the linearly polarized two-color field case ($\theta = 0.0~\pi$), the harmonic cutoff is at 104th order. However, the modulation structure on the harmonic spectrum is too large to support an isolated attosecond pulse. Besides, there is presence of multi-plateau. On increasing the polarized angle θ to 0.2π , 0.3π , 0.4π and 0.5π we see that the harmonic cutoff decreases to 100th, 90th, 84th and 71th, respectively. Moreover, the harmonic yields also decrease which is unbeneficial to the attosecond pulse generation. Besides, the harmonic plateaus become smooth and multi-plateau are eliminated. Such plateau traits favor the generation of attosecond pulses.

The smoothing of harmonic plateaus and the elimination of multi-plateau structures when increasing the polarization angle difference can be attributed to the interference effects and the dynamics of electron trajectories in HHG. On increasing the polarization angle difference, the electron trajectories that contribute to the harmonic generation become more varied. This leads to a broader distribution of electron paths, which in turn causes the harmonics to interfere with each other more destructively. As a result, the sharp features of the multi-plateau structure are smoothed out, and the overall harmonic spectrum becomes more continuous. Moreover, the increased polarization angle difference can reduce the coherence of the electron trajectories, further contributing to the smoothing of the harmonic plateaus and the elimination of distinct multi-plateau structures [45, 46].

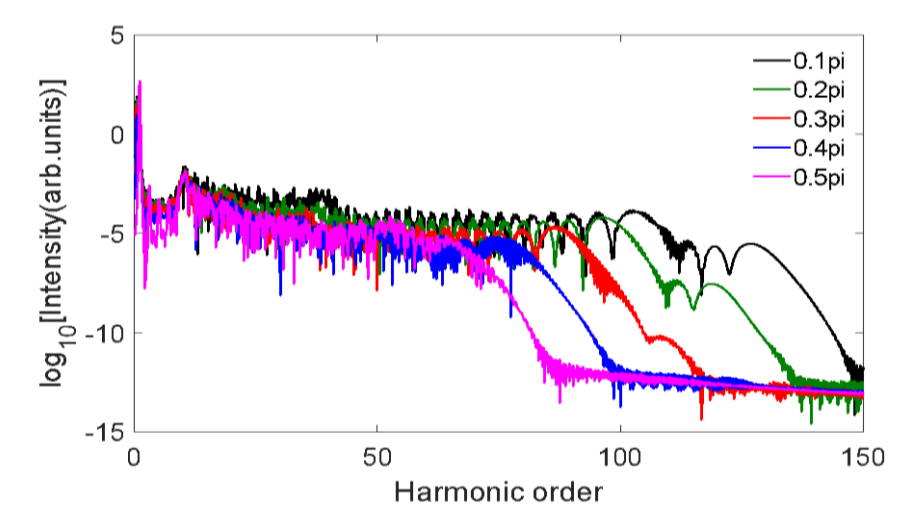


Figure 4: HHG spectra of the two-color polarized pulses with $\theta = 0.1\pi$ (solid black line), 0.2π (solid green line), 0.3π (solid red line), 0.4π (solid blue line) and 0.5π (solid pink line).

To better understand the effect of the polarization angle in the two-color field, we present the electric field in Figs. 5. A-B-C and A'-B'-C' represent the laser field processes. In Fig. 5 (a), it is clear that the A'-B'-C' process in a linearly polarized two-color field ($\theta = 0.1 \pi$) is enhanced in comparison with the A-B-C process in the one-color field. This can be attributed to intensity enhancement in the two-color field, making the electrons gain extra kinetic energy and spend more time in the acceleration and re-collision processes. This, in turn, leads to the extension of the cutoff position. When the polarization angle is $\theta = 0.3 \pi$, the processes A'-B'-C' and A-B-C in x and y components, respectively, the synthesized laser field becomes weaker [Fig. 5 (b)] than in a linearly two-color field [see Fig. 5 (a)]. This leads to suppression of the maximum harmonic emission in x and y components. On further increasing the polarization angle to $\theta = 0.5 \pi$ processes A'-B'-C' and A-B-C in x and y components, respectively, are further suppressed [Fig. 5 (c)].

When the polarization angle between the two pulses increases, the overlap of their electric fields along the x-axis decreases. This results in a lower effective intensity of the combined field

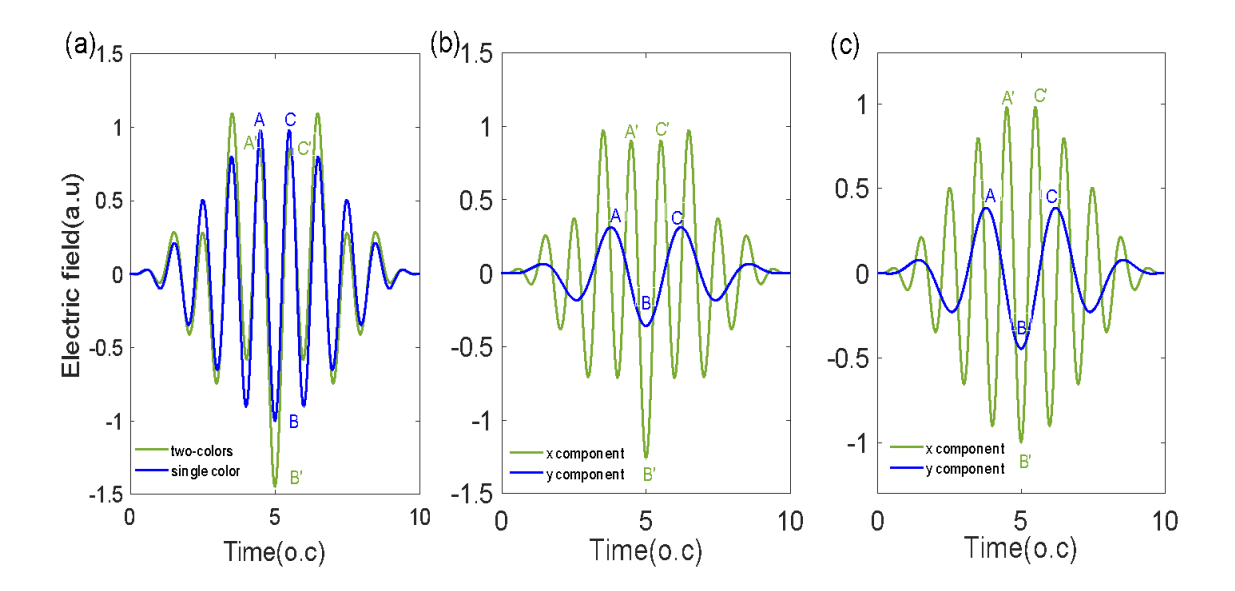


Figure 5: (a) The electric field of the single-color pulse 10 fs/800 nm (blue solid line) and the two-color pulse 10 fs/800 nm and 10 fs/2000 nm (green solid line) with $\theta = 0.0 \pi$. (b) The electric field of two-color pulse with $\theta = 0.3 \pi$ in x (green solid line) and y (blue solid line) components. (c) The electric field of two-color pulse with $\theta = 0.5 \pi$ in x (green solid line) and y (blue solid line) components.

in that direction. Since the cut-off frequency in HHG is directly related to the intensity of the driving laser field, a decrease in the effective intensity leads to a lower cut-off frequency. The y component of the control pulse can significantly influence the high-order harmonic generation (HHG) process. When the polarization angle between two pulses is adjusted, the y component of the control pulse can affect the electron trajectories and the overall dynamics of the HHG process.

CONCLUSION

The effect of polarization angle on high-order harmonic generation has been theoretically demonstrated. The results show that by using a two-color field, the cutoff point increased by 20 orders higher than in a one-color field. This is further enhanced via the introduction of inhomogeneous fields. A broad supercontinuum of approximately 270 orders was achieved at 0.003 inhomogeneity parameter. However, the introduction of polarization angle between the two fields-controlled electron dynamics as they recombined with the parent ion. This led to a decrease of the supercontinuum as the angle increased from 0.0π to 0.5π . In addition, the harmonic yield decreased, thus limiting the application of attosecond pulses. Although the study is theoretical, the findings align with trends observed in experimental HHG using tailored two-color fields and near-field enhancement from nanostructures. The predicted supercontinuum generation and polarization sensitivity can, in principle, be tested in laboratory settings using plasmonic antennas, waveguides, or gas-phase HHG experiments with polarization-tunable drivers. This demonstrates both the practical feasibility of the approach and its potential for guiding the development of optimized HHG sources for ultrafast spectroscopy.

DECLARATION

Ethics approval and consent to participate

Not applicable.

AVAILABILITY OF DATA AND MATERIALS

All the data is available on the manuscript

COMPETING INTERESTS

The authors declare that they have no conflict of interest.

FUNDING

Not applicable.

AUTHORS' CONTRIBUTIONS

Stephen Maina Njoroge conceived the idea and scheme. Stephen Maina Njoroge performed the simulations, analyzed the results and wrote the manuscript.

ACKNOWLEDGEMENTS

The authors appreciate Karatina University.

AUTHORS' INFORMATION

Not applicable.

REFERENCES

- Ciappina, M.F., et al., *Attosecond physics at the nanoscale*. Reports on Progress in Physics, 2017. **80**(5): p. 50.
- Batani, D., et al., *Atoms, solids, and plasmas in super-intense laser fields.* 2012: Springer Science & Business Media.
- Wang, Q. and Zhang, H.L. eds., *Two-dimensional Materials for Nonlinear Optics: Fundamentals, Preparation Methods, and Applications*. 2023: John Wiley & Sons.
- Finke, O., Vábek, J., Nevrkla, M. et al. *Phase-matched high-order harmonic generation in pre-ionized noble gases*.2022 Sci Rep 12, 7715. https://doi.org/10.1038/s41598-022-11313-6
- 5 Teichmann, S.M., et al., 0.5-keV Soft X-ray attosecond continua. Nature Communications, 2016. 7.
- Zijuan W., Xize G., Xiangyu M., Zhengyan L., Qingbin Z., Pengfei L., and Peixiang L.. *High Harmonic Extreme Ultraviolet Light Source with High Repetition Rate and Power*. Chinese Journal of Lasers, 2024, 51(7): 0701001
- 7 Krausz, F. and M. Ivanov, *Attosecond physics*. Reviews of Modern Physics, 2009. **81**(1): p. 163-234.
- Reinhard, J.; Wiesner, F.; Sidiropoulos, T.; Hennecke, M.; Kaleta, S.; Späthe, J.; Abel, J. J.; Wünsche, M.; Schmidl, G.; Plentz, J.; Hübner, U.; Freiberg, K.; Apell, J.; Lippmann, S.; Schnürer, M.; Eisebitt, S.; Paulus, G. G.; Fuchs, S. Soft X-Ray Imaging with Coherence Tomography in the Water Window Spectral Range Using High-Harmonic Generation. arXiv 2025. https://doi.org/10.48550/ARXIV.2503.04276.
- 9 Corkum, P.B.J.P.R.L., *Plasma perspective on strong field multiphoton ionization*. 1993. **71**(13): p. 1994.
- Johnson A. S., Avni T., Larsen E. W., Austin D. R. and Marangos J. P. *Attosecond soft X-ray high harmonic generation*. 2019. Phil. Trans. R. Soc. A.37720170468. http://doi.org/10.1098/rsta.2017.0468
- Hong, W., et al., *Method to generate directly a broadband isolated attosecond pulse with stable pulse duration and high signal-to-noise ratio.* Physical Review A, 2008. **78**(6).

- Brugnera, L., et al., *Trajectory Selection in High Harmonic Generation by Controlling the Phase between Orthogonal Two-Color Fields.* Physical Review Letters, 2011. **107**(15).
- Hutchison, C., et al., *Electron trajectory control of odd and even order harmonics in high harmonic generation using an orthogonally polarised second harmonic field.* Journal of Modern Optics, 2014. **61**(7): p. 608-614.
- Yuan, H., et al., Generation of isolated attosecond pulses in a multi-cycle inhomogeneous two-color field without CEP stabilization. Optical and Quantum Electronics, 2017. **49**(6).
- Piccoli, R., Brown, J.M., Jeong, YG. et al. *Intense few-cycle visible pulses directly generated via nonlinear fibre mode mixing*. 2021. Nat. Photon. **15**, 884–889. https://doi.org/10.1038/s41566-021-00888-7.
- Essen, P., Keijzer, B., Horen, T., Molinero, E., Galán, Á., Silva, R., and Kraus, P. *Spatial polarization gating of high-harmonic generation in solids*. 2024. 10.48550/arXiv.2409.02535.
- Roscam Abbing, S.D.C., Kuzkova, N., van der Linden, R. et al. Enhancing the efficiency of high-order harmonics with two-color non-collinear wave mixing in silica. 2024. Nat Commun **15**, 8335. https://doi.org/10.1038/s41467-024-52774-9
- Hai-Yan, S., Ai-Yuan, H., Guang-Xian, X., and Chang-Long, X. *The enhancement of high-order-harmonic generation in two-color laser field in fibonacci quasicrystals*. 2025. Optics Communications, **591**, 132135. https://doi.org/10.1016/j.optcom.2025.132135.
- Navarrete, F., and Thumm, U. Two-color-driven enhanced high-order harmonic generation in solids. 2020. Phys. Rev. A **102** (6) 063123. https://link.aps.org/doi/10.1103/PhysRevA.102.063123.
- Feng, L., M. Yuan, and T. Chu, *Attosecond x-ray source generation from two-color polarized gating plasmonic field enhancement.* Physics of Plasmas, 2013. **20**(12).
- Njoroge, S.M., et al., Control of the polarization direction of isolated attosecond pulses using inhomogeneous two-color fields. Scientific Reports, 2019. **9**(1): p. 18582.
- Petrakis, S., Bakarezos, M., Tatarakis, M. et al. *Electron quantum path control in high harmonic generation via chirp variation of strong laser pulses*. 2021. Sci Rep 11, 23882. https://doi.org/10.1038/s41598-021-03424-3
- Liu, H., Wang, Y., Zhou, S. et al. *Chirp duration effect on high-order harmonic spectra*. 2021. Eur. Phys. J. D **75**, 292. https://doi.org/10.1140/epjd/s10053-021-00302-5
- 24 Chenyang. C., Yingchun. G., and Bingbing. W. *Understanding Effects of Static Electric-field on High-order Harmonic Generation of O₂ Molecules.* 2024. Acta Photonica Sinica. **53**(6): 0653205
- 25 Bánhegyi, B., Tóth, L., Dombi, P. et al. *Controlling Plasmonic Field Enhancement via the Interference of Orthogonal Plasmonic Modes*. 2024. Plasmonics 19, 2953–2960. https://doi.org/10.1007/s11468-024-02212-9
- Shaaran, T., M.F. Ciappina, and M. Lewenstein, *Quantum-orbit analysis of high-order-harmonic generation by resonant plasmon field enhancement.* Physical Review A, 2012. **86**(2).
- Hu Q, Yang K, Li Q, Sun J, Ding Z. *Plasmon-Enhanced High-Order Harmonic Generation of Open-Ended Finite-Sized Carbon Nanotubes with Vacancy Defects*. 2024. Crystals. **14**(2):115. https://doi.org/10.3390/cryst14020115
- Wu, X., Liang, H., Kong, X., Gong, Q. and Peng, L. Enhancement of high-order harmonic generation in two-dimensional materials by plasmonic fields. 2021. Phys. Rev. A **103** (4) 043117. https://link.aps.org/doi/10.1103/PhysRevA.103.043117
- Ciappina, M.F., et al., *Attosecond physics at the nanoscale*. Reports on Progress in Physics, 2017. **80**(5).
- Kim, S., et al., *High-harmonic generation by resonant plasmon field enhancement*. Nature, 2008. **453**(7196): p. 757-60.
- Han S. Gold-sapphire Plasmonic Nanostructures for Coherent Extreme-ultraviolet Pulse Generation. 2022. Curr. Opt. Photon. 6:576-582. https://doi.org/10.3807/COPP.2022.6.6.576
- Park, D. J., & Ahn, Y. H. *Ultrashort field emission in metallic nanostructures and low-dimensional carbon materials*. 2020. Advances in Physics: X, **5**(1), 1726207.
- 33 Kim, S., et al., *Kim et al. reply.* 2012. **485**(7397): p. E1.

- Vismarra, F., Fernández-Galán, M., Mocci, D. et al. *Isolated attosecond pulse generation in a semi-infinite gas cell driven by time-gated phase matching*. 2024. Light Sci Appl 13, 197. https://doi.org/10.1038/s41377-024-01564-5
- Lv W, Wang F, Gao C. *An Effective Method for Generating Isolated Attosecond Pulses from a Solid Crystal Film.* 2024. Photonics. **11**(12):1154. https://doi.org/10.3390/photonics11121154
- Zhang, S. W., Xiao-Xin H., Yun-He X., Feng W., and Xue-Shen L. *Generation of ellipticity-tunable isolated attosecond pulses from diatomic molecules in intense laser fields.* 2023. Optics Communications. 530. 129152. https://doi.org/10.1016/j.optcom.2022.129152
- Huang, P.-C., et al., *Polarization control of isolated high-harmonic pulses*. Nature Photonics, 2018. **12**(6): p. 349-354.
- 38 Xia, C.-L. and X.-Y. Miao, Generation of Linear Isolated Sub-60 Attosecond Pulses by Combining a Circularly Polarized Pulse with an Elliptically Polarized Pulse. Chinese Physics Letters, 2015. 32(4).
- Li, M.Z., Xu, Y., Jia, G.R. and Bian, X. B. Controlling polarization of high-order harmonic generation by molecular alignment in a bicircular laser field. 2019. Phys. Rev. A. **100** (3) 033410. https://link.aps.org/doi/10.1103/PhysRevA.100.033410
- 40 Yavuz, I., et al., Generation of a broadband xuv continuum in high-order-harmonic generation by spatially inhomogeneous fields. Physical Review A, 2012. **85**(1).
- 41 Perez-Hernandez, J.A., et al., *Beyond Carbon K-Edge Harmonic Emission Using a Spatial and Temporal Synthesized Laser Field.* Physical Review Letters, 2013. **110**(5).
- Feit, M.D., J.A. Fleck, and A. Steiger, *Solution of the Schrödinger equation by a spectral method.* Journal of Computational Physics, 1982. **47**(3): p. 412-433.
- de Bohan, A., et al., *Phase-dependent harmonic emission with ultrashort laser pulses*. J Physical review letters, 1998. **81**(9): p. 1837.
- Carrera, J.J., X.-M. Tong, and S.-I.J.P.R.A.A. Chu, Molecular, *Creation and control of a single coherent attosecond xuv pulse by few-cycle intense laser pulses*. J Physical Review A—Atomic, Molecular, Optical Physics, 2006. **74**(2): p. 023404.
- 45 Yu, C., H. Iravani, and L.B. Madsen, *Crystal-momentum-resolved contributions to multiple plateaus of high-order harmonic generation from band-gap materials.* Physical Review A, 2020. **102**(3): p. 033105.
- Ngoko Djiokap, J.M. and A.F. Starace, *Origin of the multiphoton-regime harmonic-generation plateau structure.* Physical Review A, 2020. **102**(1): p. 013103.